

Efficient Spin Injector Scheme Based on Heusler Materials

Stanislav Chadov,^{1,*} Tanja Graf,¹ Kristina Chadova,² Xuefang Dai,¹ Frederick Casper,¹
Gerhard H. Fecher,¹ and Claudia Felser¹

¹*Institut für Anorganische und Analytische Chemie, Johannes Gutenberg–Universität, 55099 Mainz, Germany*

²*Department Chemie und Biochemie, Ludwig Maximilians–Universität, 81377 München, Germany*

(Received 30 March 2011; published 18 July 2011)

We present a rational design scheme intended to provide stable high spin polarization at the interfaces of the magnetoresistive junctions by fulfilling the criteria of structural and chemical compatibilities at the interface. This can be realized by joining the semiconducting and half-metallic Heusler materials with similar structures. The present first-principles calculations verify that the interface remains half-metallic if the nearest interface layers effectively form a stable Heusler material with the properties intermediately between the surrounding bulk parts. This leads to a simple rule for selecting the proper combinations.

DOI: 10.1103/PhysRevLett.107.047202

PACS numbers: 85.75.-d, 71.20.-b, 75.47.Np

New spintronic devices such as magnetoresistive random access memory or readout heads of hard disk drives [1,2] require materials exhibiting the thermally stable high degree of spin polarization needed for efficient spin injection [3,4]. A rich source is the half-metals (HMs) provided by the family of Co₂-based Heusler materials [5,6]. Nowadays they are the key candidates for the tunneling magnetoresistive (TMR) and giant magnetoresistance (GMR) devices, with two HM leads sandwiching a semiconductor (SC), insulator or nonmagnetic metal spacer layer. The amazingly high TMR ratios of 570% at 2 K were reported for the system with a HM electrode of Co₂MnSi with a AlO_x barrier [7]. However, these values are substantially reduced at higher temperatures by the magnon scattering [8]. Besides thermal activation of magnons other sources for spin depolarization are the various nonstoichiometries [9], interfacial atomic disorder [10], oxidation, spin scattering on defects [11,12], and even the intrinsic electron correlation effects [13].

Most of the significant depolarizing mechanisms are directly or indirectly caused by mechanical factors, i.e., by the lattice mismatch of HM and SC materials. By improving the quality of the interface, e.g., by choosing the materials with well-matching lattice constants, these mechanisms can be substantially reduced. For example, utilizing MgO as a barrier material and Co₂FeAl_{0.5}Si_{0.5} as an electrode, the TMR ratios of 175% could be achieved at room temperature by now [14]. On the other hand, even for the well-matching interfaces at low temperatures the severe problems could be caused by the localized interface states which couple to the bulk states of the HMs and contribute to the transport [15,16]. For example, the significant loss of spin polarization occurs on Co₂MnGe/GaAs and Co₂CrAl/GaAs interfaces [17,18] as well as on the free surfaces. Among the rare exclusions is the surface of the Mn-terminated Co₂MnSi thin film where the HM state is preserved due to the strong surface-subsurface coupling [19]. In this context the importance of studies focusing on

half-metallic properties of the interface is crucial for designing new efficient spin-injecting devices.

The extremely wide range of electronic properties and rather similar geometry exhibited by the Heusler family provides a straightforward way to construct the whole spintronic device by using only Heusler building blocks. For example, the first-principles calculations [16] for Co₂CrAl(Si)/Cu₂CrAl(001) Heusler GMR junctions predicted a spin polarization of about 80%. In the following we propose a systematic scheme to search for such proper pairs of Heusler materials for TMR/GMR junctions and justify it by the first-principles band structure calculations.

The suitable combinations can be derived from the same parent material. By making various mixtures one can produce a series of new Heusler materials with smoothly varying electronic properties ranging from half-metallic, magnetic to semiconducting and nonmagnetic. Very helpful in such a design is the so-called Slater-Pauling rule [20,21], which states the linear dependency of the unit cell magnetic moment as a function of the valence electrons number.

We will sketch our idea in detail with an example of the well-known Heusler Co₂MnAl [22] which fulfills the basic requirements of an efficient spin-injecting material. Band structure calculations [23,24] characterize it as the HM ferromagnet with a magnetic moment of $4\mu_B$ in agreement with experiment. Its measured Curie temperature is $T_C = 698$ K [25,26]. In order to derive a SC material with a similar lattice it is enough to substitute one Co atom with V. It can be synthesized, for example, by a 50-50 mixing of Mn₂VAl [27] and Co₂VAl [28]. The resulting CoMnVAl (SC) compound with 24 valence electrons is nonmagnetic in agreement with the Slater-Pauling rule [29]. The unit cells and corresponding calculated bulk band structures of both Co₂MnAl and CoMnVAl are shown in Fig. 1.

To verify which sequence of stacking layers conserves the half-metallicity, we perform the corresponding band

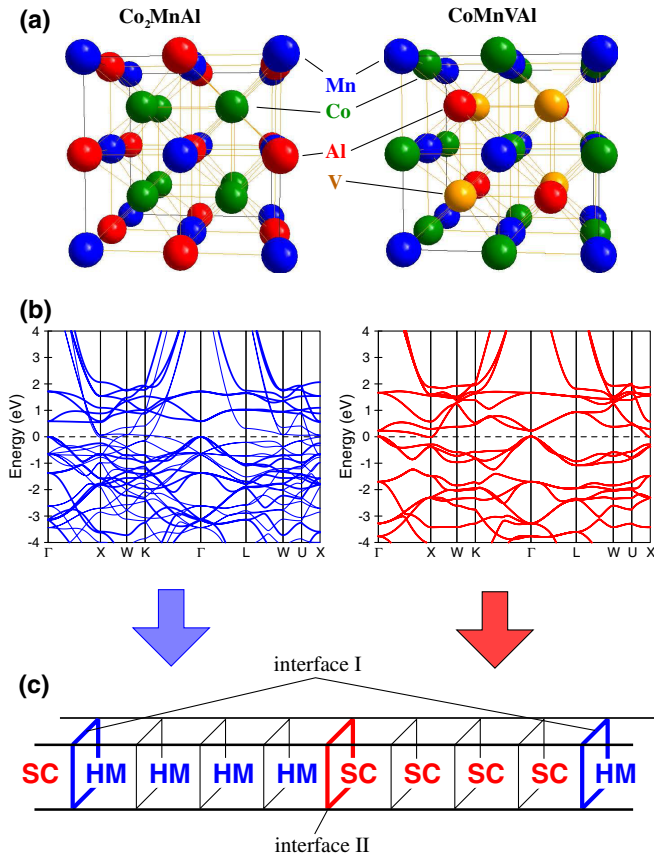


FIG. 1 (color online). (a) Crystal structures of the typical candidate materials: the half-metallic ferromagnet Co_2MnAl and the nonmagnetic semiconductor CoMnVAl . (b) Their calculated bulk band structures. In case of Co_2MnAl the bands of the gapped minority-spin channel are made thicker. The Fermi level is marked by the dashed line. (c) Structure of the supercell. Subsections marked as HM or SC represent the complete Heusler blocks, each containing four atomic layers.

structure calculations for the $\text{Co}_2\text{MnAl}/\text{CoMnVAl}$ interfaces. In the following example the stacking direction between CoMnVAl and Co_2MnAl is chosen along the densely packed (001) plane as shown on Fig. 1(b). Since the supercell contains an integer number of these units, in general it has no inversion center. For this reason one deals with two nonequivalent interfaces within each supercell. There are four stacking possibilities along the (001) plane which can be paired in two different supercells. The first one will contain Co-Co/V-Al and Mn-Al/Co-Mn, and the second Co-Co/Co-Mn and Mn-Al/Al-V interfaces. Of course, to avoid the interaction between the interfaces the supercell must be made as large as possible. For this reason all calculations were performed using the fast *ab initio* linear muffin-tin orbitals [30] method which accurately calculates the band structure within ~ 1 Ry of the Fermi energy. This allows us to study the reasonably large supercell containing 64 atoms arranged within 32 atomic layers. The exchange-correlation potential is treated using the Vosko-Wilk-Nusair form of the local spin-density approximation [31]. Since the

spin-orbit coupling is sufficiently small in these systems, the calculations are performed in the scalar-relativistic regime.

The optimization of the supercell volume yields a lattice constant nearly equal to the average of the optimized bulk values for the HM and SC materials which mismatch by about 2%. The maximal size of the supercell $(\text{CoMnVAl})_4/(\text{Co}_2\text{MnAl})_4$ (64 nonequivalent atoms arranged within 32 atomic planes) is already enough to achieve a good agreement of the layer-resolved density of states (DOS) of the Fermi energy and magnetic moments of the inner layers with the corresponding bulk values.

As it follows from the spin-resolved DOS curves (Fig. 2) the spin polarization indeed depends critically on the way of stacking: independently of the system size the half-metallicity is preserved for the system with Co-Co/V-Al and Co-Mn/Mn-Al interfaces, and in the case of Co-Co/Mn-Co and Mn-Al/Al-V interfaces it is destroyed. The substantially higher total energy (by about 3 mRy) of the supercell with “destructive” interfaces indicates their relative instability. In the destructive case the minority-spin DOS at the Fermi level for the larger $(\text{HM})_4/(\text{SC})_4$ supercell is noticeably lower than for the smaller one, $(\text{HM})_1/(\text{SC})_1$. This obviously tells us that the destructive states originate locally from the interface layers. This can be viewed in more detail by considering the layer-resolved $\text{DOS}(E_F)$ and the magnetization profiles (Fig. 3).

At Co-Co/V-Al (a), and Co-Mn/Mn-Al (b) interfaces, the spin polarization increases. At the same time at Co-Co/Mn-Co (e) and Al-V/Mn-Al (f) interfaces it is destroyed. The reason can be qualitatively understood by comparing the materials effectively formed on the interfaces with their ideal bulk equivalents, since the properties of Heuslers to a large extent originate from the nearest neighbor coupling. Indeed, Co-Co/V-Al and Co-Mn/Mn-Al interfaces correspond to the existing Heusler compounds with $2\mu_B$ magnetic moment and high spin polarization: Co_2VAl [24,27] and Mn_2CoAl [32]. As follows from Fig. 3, except for the overall demagnetization, the magnetic structure of these interfaces is rather similar to their bulk equivalents. Indeed, first of all, both interfaces are half-metallic. For the Co-Co/V-Al interface, the magnetic moments of Co atoms (0.65 and $0.5\mu_B$) are about 2 times smaller compared to the corresponding Co_2VAl bulk material (about $1\mu_B$ [28]). However, similar to the bulk, they are both positive and are followed by the nonmagnetic V-Al layer. A similar situation also occurs at the Mn-Al/Co-Mn interface: the atomic moments are approximately 2.5 , 0.78 , and $-0.68\mu_B$, compared to bulk values of about 2.69 , 0.94 , and $-1.54\mu_B$ for Mn, Co, and the second Mn, respectively [33].

The other two compounds, AlVMnAl and CoCoMnCo , which form the destructive interfaces, correspond to

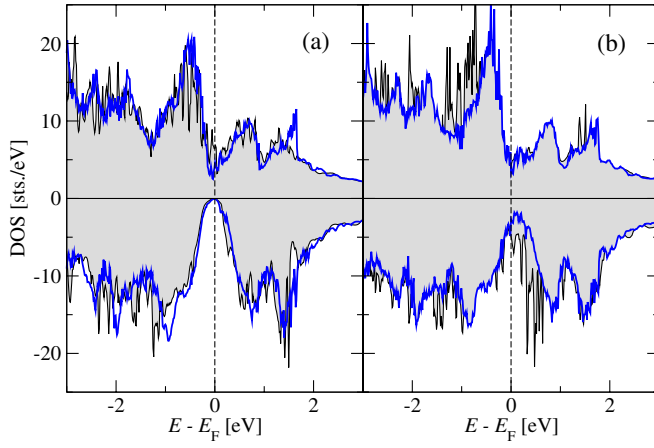


FIG. 2 (color online). Spin-resolved DOS (positive values correspond to majority-spin negative-to minority-spin channel) of the HM/SC supercells (HM = Co_2MnAl , SC = CoMnVAl) with Co-Co/V-Al, Mn-Al/Co-Mn (a) and Co-Co/Mn-Co, Mn-Al/Al-V (b) interface pairs. The gray shaded area corresponds to the minimal size of the supercell $(\text{HM})_1/(\text{SC})_1$ (scaled up by factor 4), and the thick blue curve corresponds to the largest $(\text{HM})_4/(\text{SC})_4$ supercell.

MnVAl_2 and Co_3Mn , which to our knowledge do not exist in the Heusler structure. Indeed, as we mentioned above, their calculated total energies are noticeably higher than for “constructive” interfaces and they exist mainly due to the coupling with the outer layers.

Thus we can conclude that the constructive interface (preserving the half-metallicity) can be formed if the effective interface composition would correspond to the stable bulk material with the intermediate properties between the left- and right-side materials, as in the sequence of $\text{Co}_2\text{MnAl}/\text{Co}_2\text{VAl}/\text{CoMnVAl}$ which exhibits the bulk magnetic moments of 4, 2, and 0 μ_B , respectively. The experimentally suitable method to obtain the 24-electron SC material would be through a mixture of two stable HM ferromagnets with numbers of valence electrons larger and smaller than 24.

This situation is rather general. By applying a similar first-principles analysis we have justified the analogous situation for the series of other Co_2 -based Heusler materials. The pairs of constructive and destructive interfaces were found also for $\text{Co}_2\text{MnZ}/\text{CoMnTiZ}$ ($Z = \text{Si, Ge, Sn}$) and $\text{Co}_2\text{FeZ}/\text{CoFeTiZ}$ ($Z = \text{Al, Ga}$) (more details can be found in Ref. [34]). For the constructive case the effective interface compounds will correspond to a Co_2TiZ group of half-metallic ferromagnets with magnetic moments of 1 μ_B .

The high Curie temperatures for the Co_2MnZ parent materials are known: $T_C = 685, 697,$ and 987 K for $Z = \text{Al, Ga, and Si}$, respectively [22,25,35]. The first-principles calculations [36] using a mean-field estimate [37] appear in reasonable agreement with these values (637, 698, and 1011 K, respectively). The same technique used in recent calculations [33] of the bulk Mn_2CoZ series

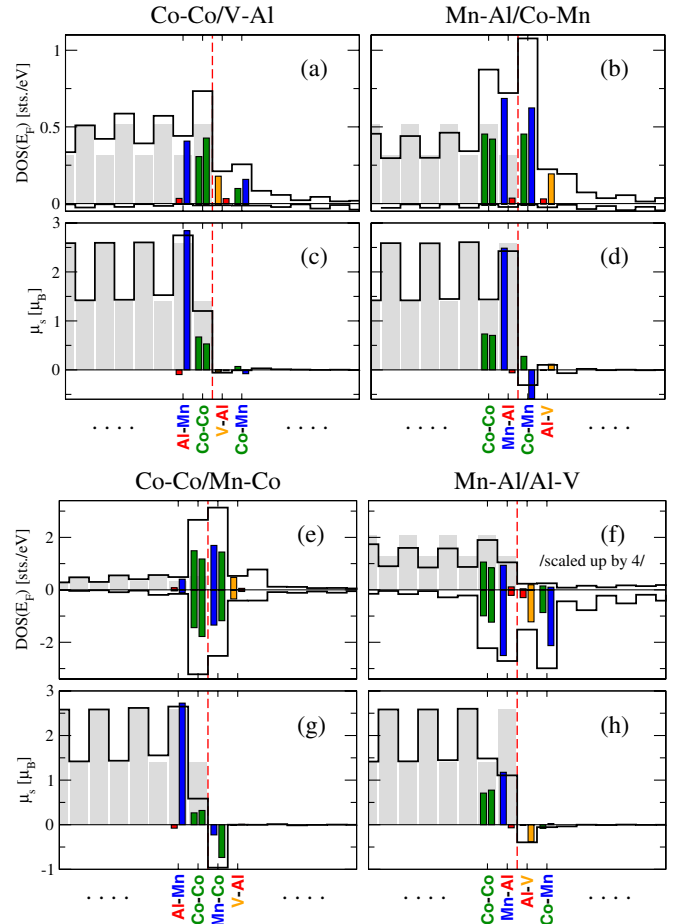


FIG. 3 (color online). The black solid line represents the layer-resolved DOS at the Fermi energy with positive values referring to the majority-spin, negative-to the minority-spin channels (a, b, e, f) and the magnetic moments (c, d, g, h) calculated for HM/SC supercells (HM = Co_2MnAl , SC = CoMnVAl). Pale gray bars show the corresponding values calculated for the bulk HM and SC materials. Darker (colored) bars mark the atom-projected contributions within the first nearest and next-nearest interface layers (each layer contains two atoms). Vertical red dashed lines mark the interface borders.

(corresponding to the effective interface compounds) predicts the $T_C = 890, 886, 578,$ and 579 K for the case of $Z = \text{Al, Ga, Si, and Ge}$, respectively. Because of the similar geometry of all constituents including the intermediate interfacial materials and thus the minimized structural distortions, together with their chemical compatibility, it is natural to expect the comparable T_C 's for the related constructive interfaces. It would be especially interesting to inspect the Curie temperatures for the Co_2TiZ or Co_2VZ junctions (experimentally or by using the mean-field estimates [37–39]) since the T_C 's of the bulk $\text{Co}_2(\text{Ti/V})\text{Z}$ systems are not high (e.g., about 140 and 350 K for Co_2TiAl and Co_2VGa , respectively [22,25,36]); however, the proximity of the high- T_C layers of the parent compounds may improve this situation.

Because of the chemical and structural compatibilities the possible disorder in constructive interfaces could be expected to be constructive as well, since it will be restricted more probably to the disorder which intrinsically occurs in the corresponding bulk systems, which are known to remain half-metallic. One of the recent examples is the $\text{CoMn}_{1+x}\text{V}_{1-x}\text{Al}$ and $\text{CoFe}_{1+x}\text{Ti}_{1-x}\text{Al}$ series ($0 < x < 0.5$) [29] which preserve the half-metallicity within the whole range. In any case, the additional detailed studies of the relative interface stabilities (as, e.g., [40]) including inspection of the various defects will be important for each constructive interface as well.

The particularly selected (001) orientation of the interfaces is also not unique. For example, we have also verified that the same rules apply for (111) orientations. This goes in line with the general idea that the most important condition is the relative smooth change of properties while going from the ferromagnetic half-metallic to a nonmagnetic semiconducting Heusler system.

Financial support by DFG Research units GSC 266 (Project Nos. P01, P07) and FOR 1464 (*ASPIMATT*) (Project No. TP 1.2-A), the BMBF (project MultiMag), and the Graduate School of Excellence MAINZ is gratefully acknowledged.

*chadov@uni-mainz.de

- [1] I. Žutić, J. Fabian, and S. D. Sarma, *Rev. Mod. Phys.* **76**, 323 (2004).
- [2] J. M. D. Coey and M. N. B. M. Venkatesan, *Lecture Notes in Physics* (Springer, Heidelberg, 2002), 595th ed., p. 377.
- [3] R. A. de Groot, F. M. Mueller, P. G. van Engen, and K. H. J. Buschow, *Phys. Rev. Lett.* **50**, 2024 (1983).
- [4] G. A. de Wijs and R. A. de Groot, *Phys. Rev. B* **64**, 020402 (2001).
- [5] J. Kübler, A. R. Williams, and C. B. Sommers, *Phys. Rev. B* **28**, 1745 (1983).
- [6] I. Galanakis, P. H. Dederichs, and N. Papanikolaou, *Phys. Rev. B* **66**, 174429 (2002).
- [7] Y. Sakuraba, M. Hattori, M. Oogane, Y. Ando, H. Kato, A. Sakuma, T. Miyazaki, and H. Kubota, *Appl. Phys. Lett.* **88**, 192508 (2006).
- [8] M. Lezaic, P. Mavropoulos, J. Enkovaara, G. Bihlmayer, and S. Blügel, *Phys. Rev. Lett.* **97**, 026404 (2006).
- [9] V. Ko, J. Qiu, P. Luo, G. C. Han, and Y. P. Feng, *J. Appl. Phys.* **109**, 07B103 (2011).
- [10] J. J. Attema, G. A. de Wijs, and R. A. de Groot, *J. Phys. D* **39**, 793 (2006).
- [11] J. Schmalhorst, S. Kämmerer, M. Sacher, G. Reiss, A. Hütten, and A. Scholl, *Phys. Rev. B* **70**, 024426 (2004).
- [12] N. D. Telling, P. S. Keatley, G. van der Laan, R. J. Hicken, E. Arenholz, Y. Sakuraba, M. Oogane, Y. Ando, and T. Miyazaki, *Phys. Rev. B* **74**, 224439 (2006).
- [13] V. Y. Irkhin, M. I. Katsnelson, and A. I. Lichtenstein, *J. Phys. Condens. Matter* **19**, 315201 (2007).
- [14] N. Tezuka, N. Ikeda, S. Sugimoto, and K. Inomata, *Appl. Phys. Lett.* **89**, 252508 (2006).
- [15] P. Mavropoulos, M. Lezaic, and S. Blügel, *Phys. Rev. B* **72**, 174428 (2005).
- [16] V. Ko, G. Han, J. Qiu, and Y. P. Feng, *Appl. Phys. Lett.* **95**, 202502 (2009).
- [17] S. Picozzi, A. Continenza, and A. J. Freeman, *J. Phys. Chem. Solids* **64**, 1697 (2003).
- [18] K. Nagao, Y. Miura, and M. Shirai, *Phys. Rev. B* **73**, 104447 (2006).
- [19] S. J. Hashemifar, P. Kratzer, and M. Scheffler, *Phys. Rev. Lett.* **94**, 096402 (2005).
- [20] J. C. Slater, *Phys. Rev.* **49**, 931 (1936).
- [21] L. Pauling, *Phys. Rev.* **54**, 899 (1938).
- [22] K. H. J. Buschow and P. G. van Engen, *J. Magn. Magn. Mater.* **25**, 90 (1981).
- [23] J. Kübler, G. H. Fecher, and C. Felser, *Phys. Rev. B* **76**, 024414 (2007).
- [24] X. Jia, W. Yang, M. Qin, and L. Wang, *J. Phys. D* **41**, 085004 (2008).
- [25] P. J. Webster, *J. Phys. Chem. Solids* **32**, 1221 (1971).
- [26] V. Jung, G. H. Fecher, B. Balke, V. Ksenofontov, and C. Felser, *J. Phys. D* **42**, 084007 (2009).
- [27] C. Jiang, M. Venkatesan, and J. M. D. Coey, *Solid State Commun.* **118**, 513 (2001).
- [28] T. Kanomata, Y. Chieda, K. Endo, H. Okada, M. Nagasako, K. Kobayashi, R. Kainuma, R. Y. Umetsu, H. Takahashi, Y. Furutani, H. Nishihara, K. Abe, Y. Miura, and M. Shirai, *Phys. Rev. B* **82**, 144415 (2010).
- [29] L. Basit, G. H. Fecher, S. Chadov, B. Balke, and C. Felser, *Eur. J. Inorg. Chem.* (to be published).
- [30] A. Perlov, A. Yaresko, and V. Antonov, “Spin-Polarized Relativistic Linear Muffin-Tin Orbitals Package for Electronic Structure Calculations, PY-LMTO.”
- [31] S. H. Vosko, L. Wilk, and M. Nusair, *Can. J. Phys.* **58**, 1200 (1980).
- [32] G. D. Liu, X. F. Dai, H. Y. Liu, J. L. Chen, Y. X. Li, G. Xiao, and G. H. Wu, *Phys. Rev. B* **77**, 014424 (2008).
- [33] M. Meinert, J.-M. Schmalhorst, and G. Reiss, *J. Phys. Condens. Matter* **23**, 116005 (2011).
- [34] C. Felser, F. Casper, X. Dai, and G. Reiss, Patent DE102008046920.3.
- [35] R. Y. Umetsu, K. Kobayashi, A. Fujita, R. Kainuma, K. Ishida, K. Fukamichi, and A. Sakuma, *Phys. Rev. B* **77**, 104422 (2008).
- [36] J. Thoene, S. Chadov, G. H. Fecher, C. Felser, and J. Kübler, *J. Phys. D* **42**, 084013 (2009).
- [37] A. I. Liechtenstein, M. I. Katsnelson, V. P. Antropov, and V. A. Gubanov, *J. Magn. Magn. Mater.* **67**, 65 (1987).
- [38] K. Sato, P. H. Dederichs, and H. Katayama-Yoshida, *Europhys. Lett.* **61**, 403 (2003).
- [39] J. Bai, J.-M. Raulot, Y. Zhang, C. Esling, X. Zhao, and L. Zuo, *Appl. Phys. Lett.* **98**, 164103 (2011).
- [40] A. Stroppa and M. Peressi, *Phys. Rev. B* **72**, 245304 (2005).